Fine-Tuning of Phase Structures and Thermoplasticity of Polyelectrolyte−Surfactant Complexes: Copolymers of Ionic Monomers with *N*-Alkylacrylamides

Markus Antonietti* and Michael Maskos

Max-Planck-Institut für Kolloid- und Grenzflächenforschung, Kantstrasse 55, D-14513 Teltow-Seehof, Germany

Received December 20, 1995; Revised Manuscript Received April 1, 1996[⊗]

ABSTRACT: Copolymers of *N*-alkylacrylamide and ionic monomers which are complexed with surfactants represent a new type of highly ordered, solid mesomorphous materials where thermomechanical behavior as well as the phase structure can be adjusted to customer-specific demands. One synthetic route toward such complexes lies in a polymer-analogous amidation of poly(acrylic acid) with tetradecylamine to various extents and subsequent complexation with cetyltrimethylammonium counterions. The behavior of these copolymers was analyzed by scattering of synchrotron radiation as well as with DSC. In these experiments, a transition from a lamellar to two different types of modulated-lamellar phases with a different cubic packing of undulations is observed. In a second set of experiments, similar materials were made by copolymerization of *N*-octadecylacrylamide and sodium 2-acrylamido-2-methyl-1-propanesulfonate and subsequent complexation of cetyltrimethylammonium counterions. The different copolymers in the series are characterized by a transition from a hexagonal to a disordered cubic morphology, depending on copolymer composition. In all cases, the degree of order of these complexes is very high, which allows some interesting applications of this new type of ordered, thermoplastic material.

I. Introduction

It is well known that ionic surfactants and oppositely charged polyelectrolytes spontaneously form addition complexes that precipitate from aqueous solution. A highly cooperative zipper mechanism which begins to operate at very low concentrations is observed, and complexes with 1:1 stoichiometry (with respect to the charges) are usually obtained (e.g., refs 1 and 2). It is important to underline that this self-assembly process, starting from simple and cheap materials and going over a very simple synthesis (common precipitation from water), directly results in very well-defined materials with a rather complex molecular structure. Our own work on polyelectrolyte−surfactant complexes was focused on the phase morphologies in the solid state of different complexes made of a variety of polyelectrolytes and diverse surfactants and lipids.[3−6] Depending on the charge density and the chemical nature of the polymer backbone and the length and shape of the surfactant, a number of lamellar or cylindrical phases were characterized. It also turned out that most of the mesophases known for block copolymers and surfactants can also be found in polyelectrolyte−surfactant complexes and that the principles of mesophase formation are closely related to the one of lyotropic phases.[7]

Due to the very high glass transitions of the ionic layers (usually above the decomposition temperature), complex films can only be organized and produced by solvent casting. For practical applications, this is a harsh restriction, and melt processing is a desirable goal. In the present paper, we wish to apply the approach of decreasing the glass transition of the ionic layer by incorporation of noncharged, polar polymeric backbone units as an internal plastiziser. To maintain a high lyotropic order as well as the stoichiometry of complex formation, a long alkyl chain should covalently be bonded to this polar repeat unit. For this purpose, we choose the *N*-alkylacrylamide repeat unit, since these monomers are stable and easily available and the amide group is expected to mix with the ionic structures of the remainder of the complex.

From a chemical point of view, the known polymer-analogous amidation of poly(acrylic acid) of known molecular weight with *N*-alkylamines to the partially substituted poly(acrylic acid)−(*N*-alkylacrylamide) copolymer is a simple way to approach the target structure. Another way toward such copolymers is copolymerization; we choose the system *N*-octadecylacrylamide (ODAA) and sodium 2-acrylamido-2-methyl-1-propanesulfonate (AMPS), since we expect an acceptable copolymerizability of both acrylamide-based monomers. In both cases, the subsequent complexation was performed with cetyltrimethylammonium counterions (CTMA). Chart 1 summarizes the chemical compositions of both sets of copolymers.

II. Experimental Section

(a) Polymer Synthesis, Complex Purification, and Film Casting. Copolymerization of different monomer ratios of 2-acrylamido-2-methyl-1-propanesulfonic acid (AMPS, Aldrich, 99%) and *N*-octadecylacrylamide (ODAA, Röhm, GmbH, 98%) was performed using 2,2′-azobis(isobutyronitrile) (AIBN, Aldrich, 98%) in a toluene/methanol mixture according to ref 8. This procedure turned out to result in the chemically most homogeneous copolymer products, as shown by sol−gel separation experiments. After a polymerization time of 12 h at 60 °C, the resulting product was precipitated from water, separated, washed, and vacuum dried at 30 °C. The compositions of the copolymers were determined by titration with aqueous potassium hydroxide solution.

The copolymer was dissolved in tetrahydrofuran (THF) with small amounts of water and subsequently neutralized with stoichiometric amounts of potassium hydroxide. Complexation of the copolymer was performed by slowly adding this solution to a stirred mixture of cetyltrimethylammonium chloride (CTMA, Aldrich, 25 wt % aqueous solution) in water. The crude copolymer complex which precipitates from aqueous solution was separated, purified by a threefold reprecipitation from THF, and vacuum dried at 50 °C. The purified product was practically free from NaCl and additional free surfactant, as shown by elemental analysis of chloride (below 0.01%). The molar compositions of the synthesized copolymers are given in Table 1.

[⊗] Abstract published in *Advance ACS Abstracts,* May 1, 1996.

S0024-9297(95)01887-0 CCC: $12.00

Table 1. Compositions of the Copolymer Complexes

copolymer complex	sample name	mol % ionic monomers[a]	mol % amidic monomer[a]	equilib water content/wt %
	CP_1-100/PAA-C_{16}	100.0	0.0	15.6
poly(hexadecyltrimethylammonium acrylate-*co*-tetradecylacrylamide)	CP_1-83	83.2	16.8	18.1
	CP_1-81	80.9	19.1	16.3
	CP_1-53	52.9	47.1	19.5
[poly(PAA/CTMA-*co*-TDAA)]	CP_1-43	43.0	57.0	12.4
	CP_1-19	18.7	81.3	10.4
	CP_1-0/PTDAA	0.0	100.0	1.4
	CP_2-100/PAMPS-C_{16}	100.0	0.0	5.3
poly(hexadecyltrimethylammonium 2-acrylamido-2-methyl-1-propanesulfonate-*co*-octadecylacrylamide)	CP_2-38	37.8	62.2	4.8
	CP_2-25	24.6	75.4	6.0
	CP_2-20	19.8	80.2	8.2
[poly(AMPS/CTMA-*co*-ODAA)]	CP_2-15	15.1	84.9	1.8
	CP_2-6	6.0	94.0	1.2
	$CP_2$0/PODAA	0.0	100.0	1.2

[a] Determined by titration before complexation.

Chart 1. Structures of the Two Different Series of Copolymers Examined in This Work: The First Series Consists of Varying Amounts of Tetradecylacrylamide and the Cetyltrimethylammonium Salt of Acrylic Acid, Whereas the Second Is Composed of Octadecylacrylamide and the Cetyltrimethylammonium Salt of 2-Acrylamido-2-methyl-1-propanesulfonate

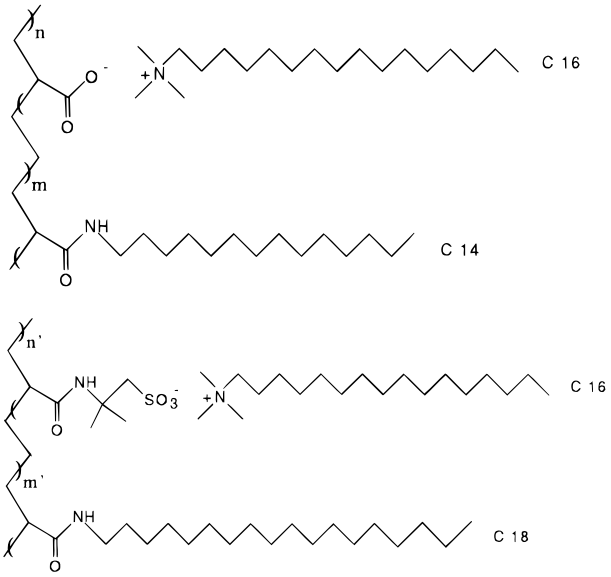

For the other set of copolymers, partially polymer-analogous amidations of PAA with tetradecylamine (TDA, Aldrich, 96%) were carried out via partial reaction of PAA with phosphorus trichloride (PCl_3, Aldrich, 98%) in dimethylformamide during 4 h at 70 °C. Slightly more than the stoichiometric amount (1.1:1) of TDA, dissolved in THF, was added dropwise. After 24 h at 70 °C, the copolymer was precipitated in water, separated, washed, and vacuum dried at 60 °C. The copolymer composition was again determined by titration with an aqueous solution of potassium hydroxide. The copolymer was dissolved in a mixture of 2-butanol, THF, and water, the stochiometric amount of potassium hydroxide was added to neutralize the acid, and this solution was slowly added to a stirred mixture of CTMA and water. The crude copolymer complex was separated, purified with a threefold reprecipitation from 2-butanol, and vacuum dried at 60 °C. Also in these cases, the purity of the products was tested with elemental analysis and turned out to be good. The molecular weight of the original poly(acrylic acid) (PAA, Aldrich) was determined by viscometry of the sodium salt in 0.1 N NaCl salt solution to be on the order of $M_v = 250\,000$; GPC measurements in aqueous buffer solutions revealed a polydispersity index of $M_w/M_n = 3$. The molar compositions of these copolymers are given in Table 1.

For film casting, a redissolution of 1 g of the solid copolymer complexes in 5 mL of THF was cast on a planar glass plate coated with octadecyltrichlorosilane. The two-dimensional geometry of the film was controlled with glass frames of variable size which are mounted on top of the glass plate. After slow evaporation of the solvent at 25 °C, the film was easily removed with the outer frame. With this procedure, the films have equilibrium water contents of up to 20% (Table 1). Complete removal of the water requires elevated temperatures ($T = 100$ °C) and the use of vacuum for ca. 12 h, but this treatment also severely changes the phase morphologies.

A Perkin-Elmer DSC 7 was used to monitor the thermal behavior of the samples.

(b) X-ray Scattering (SAXS) and Synchrotron Measurements. The synchrotron measurements were realized at DESY (HasyLab, Polymer beamline A2) in Hamburg in an s range of $1.0 \times 10^{-2} < s < 0.7$ nm^{-1} (the scattering vector is defined as $s = 2/\lambda \sin \theta$, where 2θ is the angle between the incident and scattered light). The scattering intensities were detected by an image plate system, which was calibrated using a *cornea* specimen with known reflections. The primary beam exhibits an elliptical shape which also defines the spatial resolution to be between 1.0×10^{-2} and 3.0×10^{-2} nm^{-1}.

The setup for small-angle X-ray scattering using a Kratky camera as well as the data treatment were previously described[3,6] and are not recapitulated. Here, measurements were performed in an s range of $1.0 \times 10^{-2} < s < 9.0 \times 10^{-1}$ nm^{-1}; the spatial resolution depends on geometry and is of the order 1.0×10^{-2} nm^{-1}. Desmearing was performed using the method via generalized Laguerre orthogonal functions by Burger and Ruland.[9]

WAXS measurements were partly performed at DESY with synchrotron radiation. Here, an s range of $0.8 < s < 5.0$ nm^{-1} was applied. All other WAXS data were obtained with a Nonius PDS120 powder diffractometer in transmission geometry. The unique features of the diffractometer are a FR590 generator as the source of Cu Kα radiation, monochromatization of the primary beam with a curved Ge crystal, and detection of the scattered radiation with a CPS120 position-sensitive detector. The resolution of this detector is below 0.018°. For our purpose, the measured scattering intensity as a function of the scattering vector was sufficient without further data correction.

III. Results and Discussion

(a) The Poly(PAA/CTMA-*co*-TDAA) System. In the first part, the behavior of the copolymers between acrylic acid and *N*-tetradecylacrylamide complexed with CTMA counterions [poly(PAA/CTMA-*co*-TDAA)] is discussed. Table 2 summarizes the DSC data of the complete set of complexes.

We observe that the pure PAA−CTMA complex is a material with a high tendency toward side chain crystallization. The addition of the TDAA significantly reduces the melting point as well as the crystallinity.

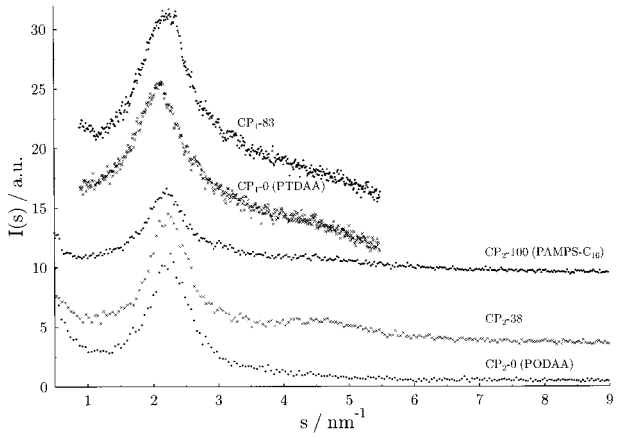

Figure 1. WAXS diffractograms of five copolymers belonging to both sets discussed in this work. The two upper curves are taken from time slices of synchrotron scattering, and the others from our standard WAXS setup. The peak shape is always rather similar and typical for an amorphous sample. For a definition of the scattering vector *s*, see text.

Table 2. DSC Data of the Copolymer Complexes

sample name	T_m/ °C	ΔH/ (J g^{-1})	T_g/ °C	Δc_p/ (J (g K)$^{-1}$)	heating rate/ (°C min^{-1})
CP$_1$-100/PAA-C$_{16}$	43.4	33.5			10
CP$_1$-83	41.4	17.4			20
CP$_1$-81	36.3	12.2			20
CP$_1$-53	27.4	11.0			20
CP$_1$-43	12.9	14.5			20
CP$_1$-19	11.9	10.9	85.0	0.2	10
CP$_1$-0/PTDAA	0.4	1.9	98.3	0.2	20
CP$_2$-100/PAMPS-C$_{16}$	−13.7	4.6	30.7	0.2	10
CP$_2$-38	−10.1	5.6			20
CP$_2$-25	−24.1	5.8			10
CP$_2$-20	−25.6	3.3			20
CP$_2$-15	−23.9	4.8			20
CP$_2$-6	−22.9	5.2			10
CP$_2$-0/PODAA	−23.5	8.3			10

This might be attributed to the mixing of side chains with different lengths. In addition, we observe the appearance of a glass transition for samples with high amide content. Samples CP$_1$-43 and CP$_2$-53 show a mechanical softening at temperatures around 120 °C, but the glass transition is obviously too broad to become visible in the DSC experiment. It must be underlined that the glass transition detected for the pure amide system (PTDAA) is in conflict with the literature behavior of long-chain acrylamides:[10] instead of a remarkably decreased T_g value caused by the long side chain, we observe a rather high glass transition. This is already a good indication that even the pure amide system has a microphase-separated structure where the alkyl side chains are not mixed with the high-T_g amide phase. Such a microphase-separated structure for the pure polyalkylamide is not known from the literature but has to be expected, since the liquid crystallinity of the very similar looking polymethacryloyl-*n*-acyl derivatives is well described.[11]

From the data of Table 2, we can conclude that the idea of flexibilizing the polar layer by adding significant amounts of amide groups had worked, although the influence on order still has to be tested.

Typical WAXS diffractograms of such copolymers reflecting the packing on the angstrom scale are shown in Figure 1. Generally, rather broad scattering peaks typical for ordered, but liquid alkyl phases are observed. Typical Bragg distances calculated from the peak maxima lie between 0.418 and 0.450 nm; this corresponds to

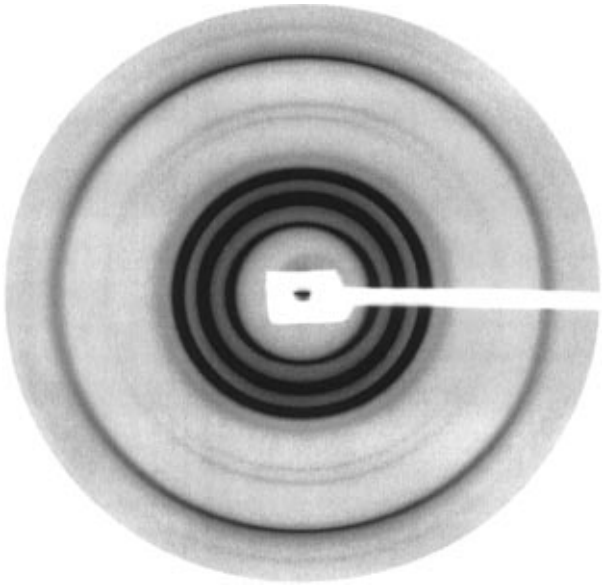

Figure 2. Raw two-dimensional scattering from the synchrotron experiment performed on the isotropic sample CP$_1$-53. No less than eight different peak sets are detected as Debye−Scherrer rings.

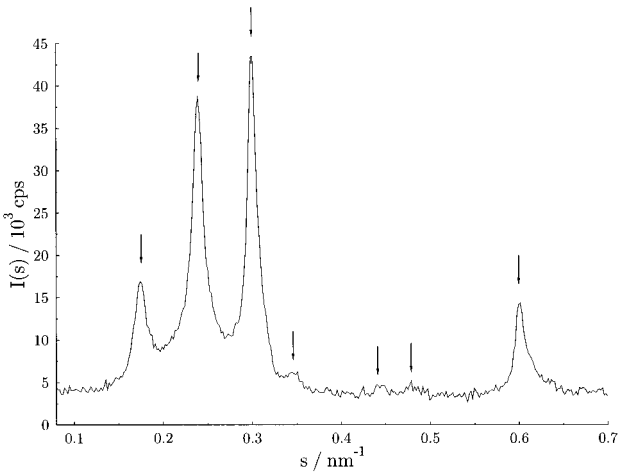

Figure 3. Vertical intersect through the two-dimensional scattering curves (as Figure 2) to evaluate the relative intensities and the widths of the peaks, here the isotropic sample CP$_1$-53. The arrows indicate the peak positions as taken from the two-dimensional recordings.

interface areas per tail of 0.202−0.234 nm^2, which also coincides with slightly ordered liquid phases.[12]

Contrary to WAXS, all small-angle experiments exhibit a very rich scattering behavior, typical for mesophases with a high degree of order. Figure 2 shows for illustration the raw two-dimensional small-angle scattering intensities of sample CP$_1$-53, as obtained from the scattering of synchrotron radiation. Even with the naked eye, no less than eight clear and rather sharp sets of scattering peaks are observed. In a mechanically untreated state, copolymer complexes are usually isotropic materials. The quality of the scattering is better judged from the horizontal intersect through the two-dimensional scattering plane, which is shown in Figure 3. Again, rather sharp peaks are observed which reflect the very high degree of order of these materials on the length scale of some nanometers. The positions of the weaker peaks are taken from the two-dimensional recording. A similar scattering behavior was observed for all complexes; Table 3 summarizes the locations of all maxima of the different complexes and a proposed

Table 3. SAXS Data of the Copolymer Complexes CP_1

sample name	peak position/nm^{-1}	corresponding dist/nm	rel ratio	proposed indexing
CP_1-100/PAA-C_{16}	0.2723	3.67	1.00	(100)
	0.5448	1.84	1.99	(200)
CP_1-83	0.1722	5.81	1.00	(100)
	0.2361	4.24	1.37	(110)
	0.2953	3.39	1.71	(111)
	0.5914	1.69	3.44	(222)
CP_1-81	0.1747	5.73	1.00	(100)
	0.2378	4.21	1.36	(110)
	0.2998	3.34	1.72	(111)
	0.3448	2.90	1.98	(200)
	0.4430	2.23	2.54	(211)
	0.4752	2.10	2.72	(220)
	0.6019	1.66	3.45	(222)
CP_1-53	0.1764	5.67	1.00	(100)
	0.2401	4.16	1.36	(110)
	0.3012	3.32	1.71	(111)
	0.3471	2.88	1.97	(200)
	0.4459	2.24	2.53	(211)
	0.4794	2.09	2.71	(220)
	0.6025	1.66	3.42	(222)
CP_1-43	0.2523	3.96	1.00	(111)
	0.3128	3.20	1.24	(200)
	0.6273	1.59	2.49	(400)
CP_1-19	0.2447	4.09	1.00	(111)
	0.2909	3.44	1.22	(200)
	0.6163	1.62	2.45	(400)
CP_1-0/PTDAA	0.2561	3.90	1.00	(111)
	0.2843	3.52	1.11	(200)
	0.4250	2.35	1.66	(220)
	0.5176	1.93	2.02	(222)
	0.5840	1.71	2.28	(400)

indexing of the peak sequences. Obviously, the symmetry within this series switches two times: PAA-C_{16} with its high degree of side chain crystallinity is a lamellar material. The long period of the layers of 3.67 nm is in the expected range and in good agreement with the values for analogous complexes between poly(styrenesulfonate) and C_{16} chains. In spite of the contour length of the tails of ca. 2 nm and an amorphous content of ca. 60%, we propose to describe PAA-C_{16} with a bilayer-like morphology. CP_1-83, CP_1-81, and CP_1-53 can be indexed according to a cubic order but also exhibit C_2 symmetry, as seen by polarization microscopy and the scattering experiments on oriented samples. In addition, the first peak occurs at comparably small angles; the related Bragg distance of 5.8−5.6 nm clearly exceeds the expected layer distance and must be related to some superstructure.

Having indications for lamellar as well as cubic elements within the physical behavior of those samples, we want to propose a structure model where all data are explained by a lamellar superstructure having localized thickness undulations which get packed in a cubic arrangement; the layer distances of $d = 3.39$ (CP_1-83), 3.34 (CP_1-81), and 3.32 nm (CP_1-53) also correspond to the strongest peak (see Figure 3) and agree with the lamellar PAA-C_{16} distance, with some minor corrections for the amorphous character. The positioning of this peak to the other peaks (indexed as (111)!) and the magnitudes indicate that the lamellae normal is parallel to the room diagonal of the cubic unit cells. An idealized, computer-generated model of this structure is shown in Figure 4a. This arrangement of unit cell and lamellae results de facto in a hexagonal packing of the undulations in each lamella (the whole phase morphology is then rhombohedric or an R_{II} phase; see ref 7. This symmetry type is very similar to a phase morphology of block copolymers which was called "hexagonally perforated layers" (HPL; see ref 13).

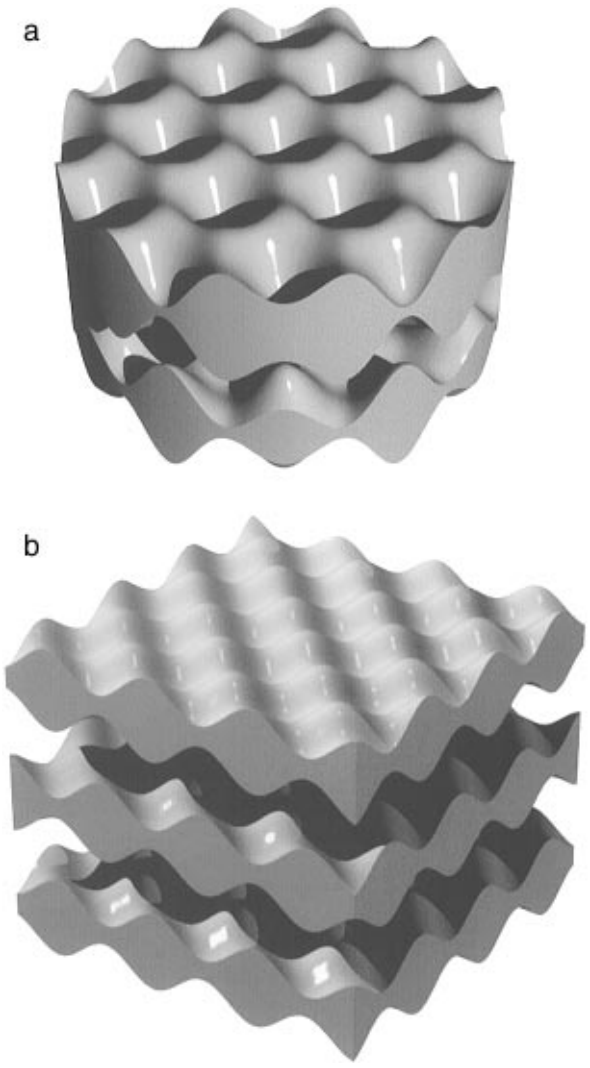

Figure 4. Illustration of the model of undulated lamellar structures which can explain the experimental findings: A fcc-cell is defined by the packing of thickness undulations. In modification a, corresponding to samples CP_1-83, CP_1-81, and CP_1-53, the lamellae are oriented along the room diagonal. In modification b, corresponding to samples CP_1-43, CP_1-19, and CP_1-0, an orientation parallel to the surface of the unit cell is preferred. Note that these structures are just idealized models; for a better clarity, the height of the wiggles are overdrawn in (a).

The scattering of samples CP_1-43 and CP_1-19 as well as the pure amide, PTDAA, can again be indexed according to a cubic order, but the number of peaks has significantly diminished, related to a higher symmetry. The peak we attribute to the distance of the lamellae is now indexed as (200), which is related to an arrangement of the lamellae parallel to the surface of the unit cell. The resulting supersymmetry is now tetragonal (or a T_{II} phase, see again ref 7). The proposed structure model is illustrated in an idealized form in Figure 4b.

The calculated layer distances are $d = 3.20$ (CP_1-43), 3.44 (CP_1-19), and 3.52 nm (PTDAA) and agree well with the d values of all other complexes of this series. Note that the undulations are now packed in a quadratic arrangement in each layer.

The difference between the two arrangements of the undulation structure observed in this sample set is not only expressed in a different symmetry but results also in a different wavelength Λ of the undulations: $\Lambda = 1.41d$ for CP_1-0 to CP_1-43 as compared to $\Lambda = 2.44d$ for CP_1-53 to CP_1-83. The different wavelength is directly

connected with the different packing of the layers and the different symmetry.

We can only speculate about the origin of these different undulation structures. A shorter wavelength is usually attributed to a higher frustration constant or a higher spontaneous curvature of the system.[14] This is in good agreement with the geometry of both polymer components, since we expect the ion pair of the surfactant complex to be larger than the amide group and the frustration is increasing with the ion content. Another source of the different interface structures might be a different segregation of both components, expressed as the thickness of the interface layer and caused by the decreasing polarity with increasing amide content.

It was stated above that all films contain a remarkable equilibrium amount of water which is required for the hydration of the head groups and structure formation. This water content depends delicately on copolymer composition and can reach values as much as 19.5%. Surprisingly, the water uptake is not related to the amount of ionic head groups but scatters in an ill-defined way over the whole set of samples. This is speculatively explained by the use of the water molecules to fit geometric imperfections of the diverse phase morphologies.

For a systematic examination of the influence of water, we carefully dried all samples at high temperature and in vacuo. In this vigorously dried state, all complexes exhibit a lamellar morphology with $d = 3.31-3.55$ nm. A quantitative data evaluation of the scattering curves reveals rather high excess surface areas (characterized by the ratio of real interface area A per projected unit area A_0), thus indicating the frustrated, but nonordered state of the interface. Time-resolving experiments where hydration/dehydration has been performed in the synchrotron beam show that the transition between the modulated lamellar state (equilibrium water) and the frustrated, disordered lamellar state (dried) is fully reversible and occurs via continuous growth or reduction of the respective peaks; i.e., there is no abrupt change of the structure with drying, and just the undulation structure vanishes and reappears with water uptake. Also, the absolute value of the water content is fully recovered.

Measurements on oriented samples which would be surely helpful to underline the proposed structure models were not considered in the current synchrotron schedule and will be presented in context with some rheooptical data and the elongation/orientation behavior in a subsequent publication.[15]

(b) The Poly(AMPS/CTMA-*co*-ODAA) System. The discussion of these copolymers is similar to that of the previous system. The thermodynamic data as obtained by DSC are included in Table 2. We observe that all samples exhibit a melting point due to side chain crystallinity well below room temperature with rather low melting enthalpies, a measure for the low partial crystallinity involved in this change. It must be underlined that even the pure PODAA, although it contains C_{18} side chains, has a melting point well below the one of the PTDAA (a member of the first series) with its C_{14} side chains. The lowering of the melting points as compared to the first copolymer family is a clear indication that these copolymers exhibit phase morphologies which back a nonparallel arrangement of the hydrophobic tails; i.e., from DSC, we expect nonlamellar morphologies. The amorphous character of the side chains at room temperature is also underlined by WAXS

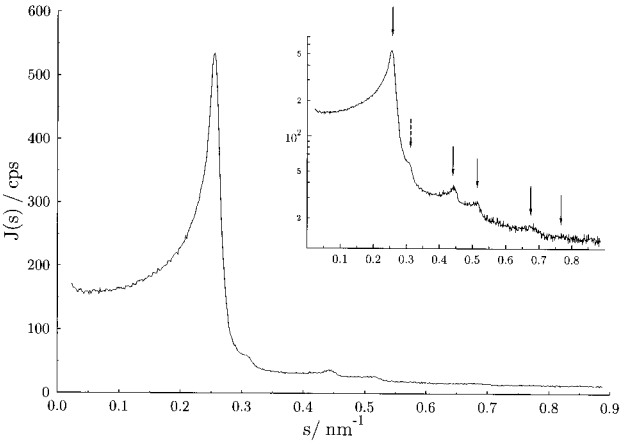

Figure 5. Smeared SAXS data of PAMPS-C_{16} in a linear and a logarithmic presentation (inlet).

Table 4. SAXS Data for the Pure PAMPS−CTMA Complex

peak position/nm^{-1}	corresponding dist/nm	rel ratio	proposed indexing
0.2607	3.84	1.00	(10)
0.3130	3.19	1.20	
0.4495	2.22	1.72	(11)
0.5197	1.92	1.99	(20)
0.6889	1.45	2.64	(21)
0.7781	1.29	2.99	(30)

data, as shown in Figure 2 for three different polymers of this series.

Polarization microscopy on oriented samples shows a high macroscopic anisometry with C_2 symmetry for the pure PAMPS-C_{16} and CP_2-38 only. All other copolymers including the pure PODAA, exhibit no peculiar birefringence induced by the ordering of the phase structures; only a minor contribution due to induced stress fields typical for glassy polymers is observed. The latter observations can be related to a cubic, a sponge-like, or a disordered phase structure.

SAXS measurements on films of the pure PAMPS-CTMA reveal a clear picture. The related scattering curve is shown in Figure 5. We observe no less than six peaks, most of which can be indexed according to a hexagonal packing of cylinders, as demonstrated in Table 4. Only the second peak cannot be explained by the hexagonal indexing, and this is speculatively attributed to a periodicity of undulations along the cylinders, too, analogous to the mesomorphous structure of PAA-C_{12}.[4] This model is supported by the scattering on oriented samples, as demonstrated in Figure 6. All hexagonal peaks are moved to a scattering plane perpendicular to the stretching direction: just the additional peak which was attributed to order onto the cylinders does not lie on the equator of the scattering plane and exhibits an intensity contribution which becomes visible as a projection parallel to the stretching direction (note that the apparent peak position has shifted by $\sqrt{2}$ as compared to the unoriented sample, which marks it as a peak being located at the diagonal).

A very similar behavior is also found for CP_2-38; up to 62 mol % ODAA in the copolymer composition, the hexagonal phase is preserved. Since CP_2-38 plasticizes at elevated temperatures, this composition range of the second series gives access to thermoplastic, hexagonal PE−surfactant complexes.

The scattering behavior changes dramatically for all systems with higher amide contents, starting with CP_2-

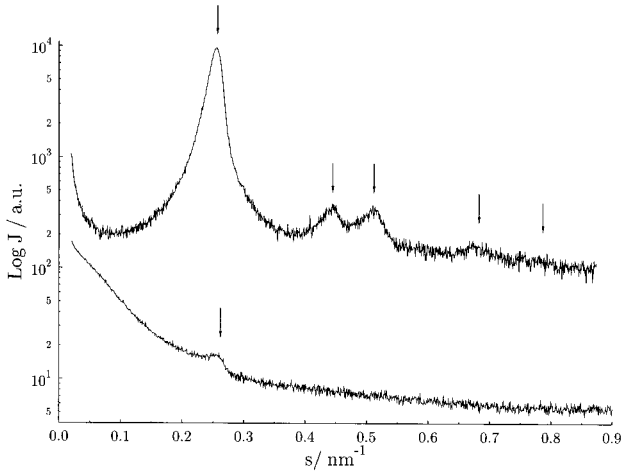

Figure 6. Comparison of the SAXS data on an oriented sample of PAMPS-C_{16} parallel and perpendicular to the stretching direction. All peaks which have been indexed according to a hexagonal packing are allocated perpendicular to stretching, which proves that the cylinders are oriented parallel to the stretching direction.

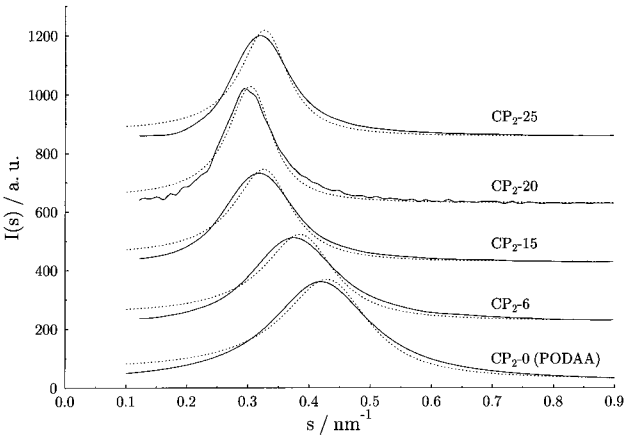

Figure 7. Desmeared SAXS data of samples CP_2-25 to CP_2-0 (the pure PODAA). A broad peak typical for spongelike structures is observed. The dotted lines indicate the fit of the data according to the Teubner−Strey model.

25. Figure 7 shows the small-angle diffractograms of these systems. In each curve, only a broad, unstructured scattering peak is observed. This scattering behavior also does not depend on orientation: the scattering curve of a highly elongated sample still is isotropic, which confirms the macroscopic orientation behavior as observed with polarization microscopy.

The shown peak shape is similar to the one of the well-known sponge phase of microemulsions or the L_3 phase of concentrated surfactant solutions.[16] We can understand the sponge phase as a bicontinuous structure with a distinct size of the structures (related to surfactant geometry), but no long-range order. The existence of such a phase in the second set of copolymeric polyelectrolyte−surfactant complexes as well as the pure PODAA polymer explains all experimental findings, i.e., the absence of macroscopically ordered domains as revealed by polarization microscopy, the scattering behavior, and the unconventionally low melting transition of the C_{18} tails.

Consequently, we have fitted the data with the Strey−Teubner formalism,[17] which approximates the bicontinuous structure with a rather simplified, but closed expression for the radial correlation function. This model was developed and successfully applied for

Figure 8. Computer model of the bicontinuous sponge phase which is postulated for all samples in the composition range between CP_2-25 and the pure PODAA.

Table 5. Parameters of the Teubner−Strey Fit of the Scattering Curves of Samples CP_2-64 to CP_2-0 (PODAA)[a]

sample	α/nm	ξ/nm	$K = 2\pi/d$	$K\xi$
Cp_2-25	3.03	6.928	2.075	14.38
Cp_2-20	3.25	7.039	1.928	13.57
Cp_2-15	3.03	5.778	2.075	11.99
Cp_2-6	2.56	5.623	2.456	13.81
PODAA	2.29	5.149	2.746	14.14

[a] ξ is the correlation length of the bicontinuous structure.

spongelike microemulsions.[18] Table 5 shows the resulting fit parameters, expressed as the averaged interdomain distance d and a correlation length ξ which determines the loss of order between the different domains; the resulting fit functions were already included in Figure 7. From the quality of the fits, it is seen that the experimental peak shape, especially the tail to large s values, is not fully described, which might be attributed to the crude approximations of the theory. The quantity d of the Strey−Teubner fits ought to be compared with a Porod length l_P, which is generally well below the length of the periodic repeat unit; the values listed in Table 5 are consequently in good agreement with geometric considerations based on the molecular architecture of the complexes. The relative correlation loss expressed as $k\xi$, on the other hand, is well below that of the analogous microemulsion data;[14] i.e., the present spongelike PE−surfactant complexes exhibit a six- to eightfold higher relative correlation length or ordering than the microemulsions systems.

A computer model of the related sponge structure of the PODAA is shown in Figure 8.

IV. Conclusion and Outlook

It has been shown that copolymers of ionic monomers and *N*-alkylacrylamides can be complexed in the complete composition range by oppositely charged surfactants, thus resulting in materials with order phenomena very similar to those of the pure polyelectrolyte−surfactant complexes. Due to this copolymerization, a decrease of the glass transition of the ionic layers down to temperatures of $T_g \sim 60$ °C is obtained, which makes these complexes thermoprocessible.

All of these complexes form highly ordered microstructures at a length scale between 3 and 6 nm, where the phase morphology delicately depends on copolymer composition. From an academic point of view, this

allows the examination of the sequence of phase structures and phase transition effects by variation of the composition, a simple chemical parameter.

For the first set of copolymers consisting of TDAA and AA/CTMA, we detect a transition from a lamellar phase to two different modulated-lamellar phases, where we try to explain all data by two different wavelengths and packing symmetries of the undulations in the interface, namely, a T_{II} and a R_{II} morphology. With respect to the layers, the packing of the undulations is in one case quadratic (with an A−B−A layer sequence), and the ratio of the undulation wavelength and the layer distance is $\Lambda = 1.41d$. In the other case, a hexagonal packing of undulations is observed, and $\Lambda = 2.44d$. This is related to a different positioning of the cubic cell (which might be constructed from the maxima of undulations) relative to the lamellae normal.

In the copolymer set of ODAA and AMPS/CTMA, a transition from a hexagonal to a bicontinuous morphology is observed. In the hexagonally ordered complexes, the occurrence of periodic undulations is also observed; this frustration effect is obviously a more general phenomenon rather than an exception in PE−surfactant complexes. All bicontinuous structures exhibit a very similar scattering pattern which can be described with the Teubner−Strey correlation function and a related spongelike structure.

Due to the different scope of the present paper, we have omitted more detailed examinations on oriented samples, which would clearly help to support the presented structure models. Since first experiments indicate that the combined elongation/orientation behavior of the modulated-lamellar phases is rather complex, we plan to combine the SAXS measurements with rheooptical experiments, which allows not only a more precise structure assignment but also a quantitative description of the degree of order on different length scales. This is the topic of a forthcoming publication.[15]

In addition, the orientationally well-defined films and pellets allow a testing of the mechanical and dielectric properties as well as the permeation of low molecular weight compounds through these microphase-separated materials as a function of the morphology. Another current topic of our research is the screening for new phases and transition phenomena by using other copolymer and surfactant structures, such as chiral surfactants and surfactant bearing chemical functionalities.

Acknowledgment. We thank C. Burger and A. Thünemann for numerous discussions and help during the synchrotron measurements and with computer graphics. Financial support by the Max Planck Society is gratefully acknowledged.

References and Notes

(1) Goddard, E. D. *Colloids Surf.* **1986**, *19*, 301.
(2) Hayagawa, K.; Santerre, J. P.; Kwak, J. C. *J. Phys. Chem.* **1982**, *86*, 3866; **1983**, *87*, 506.
(3) Antonietti, M.; Conrad, J.; Thünemann, A. *Macromolecules* **1994**, *27*, 6007.
(4) Antonietti, M.; Conrad, J. *Angew. Chem., Int. Ed. Engl.* **1994**, *33*, 1869.
(5) Antonietti, M.; Burger, C.; Effing, J. *Adv. Mater.* **1995**, *7*, 751.
(6) Antonietti, M.; Kaul, A.; Thünemann, A. *Langmuir* **1995**, *11*, 2633.
(7) Seddon, J. M. *Biochim. Biophys. Acta* **1990**, *1*, 1031.
(8) Modet, J.; Papantoniou, C.; Vanlerberghe, G. Eur. Pat. Appl. EP 406042 (*Chem. Abstr.* 61K7/06), 1991.
(9) Burger, C.; Ruland, W., presented at the IXth International Meeting on Small Angle Scattering, Saclay, 1993.
(10) Brandrup, J.; Immergut, E. H., Eds. *Polymer Handbook*, 3rd ed.; Wiley: New York, 1989.
(11) Shibaev, V. P.; Tal'roze, R. V.; Karakhanova, F. I.; Platé, N. A. *J. Polym. Sci., Polym. Chem. Ed.* **1979**, *17*, 1671.
(12) Tanford, C. *The Hydrophobic Effect*, 2nd ed.; Wiley: New York, 1980.
(13) Förster, S.; Khandpur, A. K.; Zhao, J.; Bates, F. S.; Hamley, I. W.; Ryan, A. J.; Bras, W. *Macromolecules* **1994**, *27*, 6922.
(14) Evans, D. F.; Wennerstrom, H. *The Colloidal Domain*; VCH: Weinheim, 1994.
(15) Antonietti, M.; Burger, C.; Thünemann, A., to be published.
(16) Chen, S. H.; Chang, S. L.; Strey, R.; Samseth, J.; Mortensen, K. *J. Phys. Chem.* **1991**, *95*, 7427.
(17) Teubner, M.; Strey, R. *J. Chem. Phys.* **1987**, *87*, 2195.
(18) Chen, S. H.; Chang, S. L.; Strey, R. *J. Appl. Crystallogr.* **1991**, *24*, 721.

MA9518870